A spiral-polished fiber sensor for strain and temperature measurement

Yiwei Ma[1] · Chunbo Su[1] · Yang Yi[1] · Min Zhao[1] · Jing Sun[1] · Senyu Wang[1] · Xiaoyang Li[1] · Geng Tao[1] · Shengnan Yu[1] · Chengguo Tong[2] · Weimin Sun[1] · Libo Yuan[3]

Abstract

We propose and experimentally investigate a spiral-polished single-multi-single-mode (SP-SMS) fiber sensor for the simultaneous measurement of strain and temperature. This special spiral shape on a multimode fiber is fabricated by a high-frequency CO_2 laser, which excites higher order cladding modes in the interference process and leads to high strain sensitivity. Experimental results show that the strain sensitivity for the proposed structure in the transmission spectrum of two marked interference dips is -17 pm/με and -1 pm/με in the range of 0–600 με. Moreover, temperature sensitivities of 10 pm/°C and 13.3 pm/°C are obtained in the range of 30–150 °C. Furthermore, the proposed sensor is inexpensive, is easy to fabricate and has a compact structure.

1 Introduction

Recently, strain measurement using an optical fiber sensor has been a research issue of interest in the fields of structural health monitoring, disaster forecasting and artificial intelligence [1–3]. Fiber-optic sensors have unique advantages, such as a small volume, a low weight, an easy fabrication method, strong reliability and an anti-electromagnetic interference capability [4, 5]. Various optical fiber structures for strain measurement have been proposed, such as fiber Bragg gratings (FBGs) [6], photonic crystal fiber (PCF) structures [7], long-period fiber gratings (LPFGs) [8] and multimode interferometers (MMIs) [9]. Among these, the FBG has a compact structure in length, but it suffers from a low strain sensitivity of 1 ~ 2 pm/με. The PCF sensor achieves relatively high strain sensitivity but is costly. LPFGs usually have high sensitivity and low cost. However, most LPFGs suffer from temperature–strain crosstalk because only one resonant peak can be demodulated.

Instead, multiparameter measurements are realized by optical sensors based on MMIs [10]. The basic principle of the MMI is mode coupling among different modes in an optical fiber. This interference phenomenon is widely investigated and applied in optical sensing. Hence, much research on the use of the MMI structure to measure temperature and strain simultaneously has been proposed. For example, an optical sensor is proposed for the simultaneous measurement of strain and temperature by sandwiching a polarization-maintaining fiber (PMF) between two multimode fibers (MMFs) [11]. The transmission spectrum of the sensor exhibits a high extinction ratio of 30 dB; however, the strain sensitivity of the sensor is relatively low, reaching only 1.01 pm/με and 1.27 pm/με.

A typical case of the MMI is the single-multi-single-mode (SMS) fiber structure [12]. This modal interference structure is easy to fabricate, is low cost and offers excellent sensing performance; moreover, it is capable of simultaneously measuring multiple parameters. In Ref. [13], the strain sensitivity of the sensor is enhanced to -7 pm/με and -2.19 pm/με by twisting the multimode fiber of the SMS structure. It achieves a high resolution in the measurement of strain and temperature by the spatial frequency demodulation method. However, the heating-induced preparation method of the structure is relatively imprecise, and the transmission loss of the sensor is high. Therefore, researchers must

✉ Geng Tao
gengtao_hit_oe@126.com

1   Key Lab of In-Fiber Integrated Optics, Ministry Education of China, Harbin Engineering University, Harbin 150001, China

2   Guangxi Key Laboratory of Wireless Wideband Communication and Signal Processing, Guilin University of Electronic Technology, Guilin 541004, China

3   Photonics Research Center, Guilin University of Electronics Technology, Guilin 541004, China

develop a fiber sensor that features high sensitivity, low cost and a reliable fabrication method.

In this paper, we propose and experimentally demonstrate an all-fiber sensor constructed with a spiral-polished SMS structure (SP-SMS). The spiral geometry of the fiber structure is polished by a high-frequency CO_2 laser. This design breaks the circular symmetry of the fiber and excites higher order modes in the interference process to improve the sensitivity. Experimental results show that in the dynamic range of 0–600 µɛ, the strain sensitivities of two dips at wavelengths of 1319.6 nm and 1359.8 nm are −1 pm/µɛ and −17 pm/µɛ, respectively; thus, the strain sensor exhibits a detectable resolution of 1.2 µɛ. In addition, in the temperature range of 30–150 ℃, the sensitivities of the foregoing dips are 10 pm/℃ and 13.3 pm/℃, respectively. Simultaneous measurement of the strain and temperature is achieved by monitoring the shift in the two dips in the transmission spectrum. Moreover, the proposed sensor is low cost and has a flexible preparation method; thus, it has much potential in the optical fiber sensing field.

2 Fabrication and principle

Figure 1 shows a schematic diagram of the SP-SMS structure. The length of the MMF section is 2.5 cm, and a continuous spiral groove of 2 cm is polished on it. The experimental system for preparing the spiral-polished SMS structure is exhibited in Fig. 2. An optical broadband source (BS) and an optical spectrum analyzer (OSA, YOKOGAWA, AQ6370D) with a resolution of 0.02 nm are employed to provide incident light and analyze the light signal, respectively. A high-frequency CO_2 laser with an output power of 10 W is employed to polish the optical fiber structure. Three steps are performed to prepare the spiral-polished fiber sensor. First, we use a highly precise fiber splicing system [15] to fabricate the SMS structure. A step-index MMF (AFS62.5/125Y) of 2.5 cm is spliced with two standard single-mode fibers (SMFs, Corning 28).

Then, the SMS structure is fixed in the middle of the two fiber fixtures and connected to the BS and OSA, and
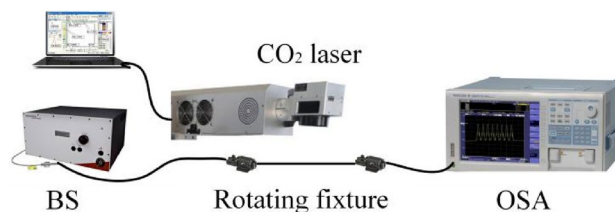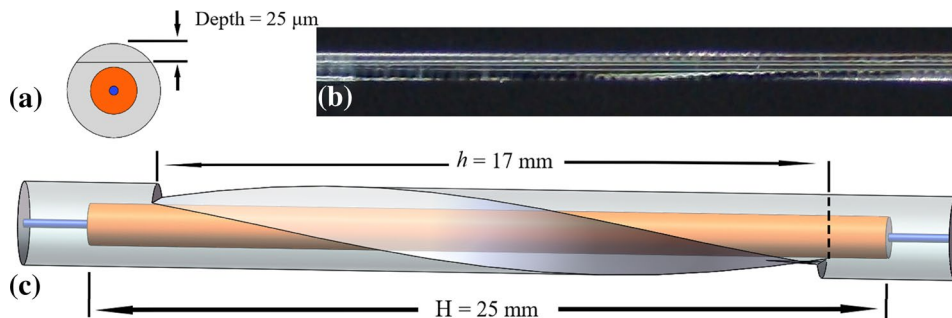
Fig. 2 Experimental devices for fabricating the spiral-polished SMS structure

the distance between the two fiber fixtures is 17 cm. The fiber fixtures are rotated to twist the SMS structure into five circles. Afterwards, the laser is turned on to polish the middle twisted MMF. The scanning path of the laser is programmed by computer software, which can polish the optical fiber continuously. The diameter of the focal spot of the CO_2 laser is 100 µm, and the pulse scanning speed and the pulse frequency are 100 m/s and 30 kHz, respectively. The polished length of the fiber is 2 cm, the polishing power is set as 1.5 W, and the polishing process is repeated twice. Cladding with a depth of 25 µm is removed, and a polished depth of 25 µm is selected to maintain mechanical strength and a relatively low transmission loss. As a result, a spiral-polished SMS structure is successfully prepared, which is shown in Fig. 1b. Figure 3 shows the transmission spectrum of the SP-SMS and original SMS. Dip A (1317 nm) and Dip B (1359 nm) are marked as the dips of interest in this research, and Dip C and Dip D are the interference dips of the original SMS.

When the incident light $E(r, 0)$ propagates to the SMS structure, the two splicing points of the MMF function as the mode spitter and mode coupler. The field profile of the incident light is expressed as:

$$E(r,\ 0) = \sum_{m=1}^{M} c_m F_m(x, y), \tag{1}$$

where $F_m(r)$ is the electric field distribution of the eigenmodes within the MMF, which depends on the core diameter of the MMF. c_m is the excitation coefficient, which is obtained by the following equation:
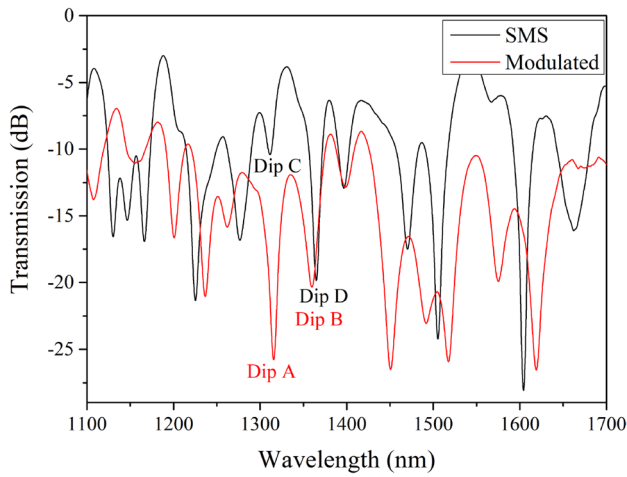
Fig. 1 Schematic diagram of the proposed fiber structure and side view of the SP-SMS

Fig. 3 Transmission spectra of the original SMS structure and modulated spiral structure

$$c_m = \frac{\int_0^\infty \int_0^\infty E(x,\, y, 0) F_m(x, y) dx dy}{\int_0^\infty \int_0^\infty F_m(x, y) F_m(x, y) dx dy}. \tag{2}$$

Therefore, the light field inside the MMF at a propagation length of z is deduced as

$$E(x, y,\, z) = \sum_{m=1}^{M} c_m F_m(x, y) exp(i\beta_m z), \tag{3}$$

where β is the propagation constant of the m-th-order modes of the MMF [14].

The phase difference ϕ between the core mode and cladding mode is approximated as [16]:

$$\phi = \frac{2\pi \Delta n_{eff} L}{\lambda}, \tag{4}$$

where Δn_{eff} is the refractive index difference between the core and cladding mode and L is the interference distance. When the phase difference satisfies $\phi = (2m + 1)\pi, m = 0, 1, 2...$, the interference dip λ_m of the structure in the transmission spectrum is expressed as follows:

$$\lambda_m = \frac{2\Delta n_{eff} L}{2m + 1}, \quad m = 0,\, 1,\, 2... \tag{5}$$

Due to the thermal effect of the CO_2 laser, when the laser pulse is released, dense heat will induce the gasification of SiO_2; thus, the glass on the surface of the fiber will be removed. In addition, residual stress release occurs in this process, which will induce a refractive index (RI) change. The effective RI of the fiber core ($n_{eff,co}$) will be decreased; thus, more light will travel to the cladding, and the higher order modes will more likely be excited in this process,
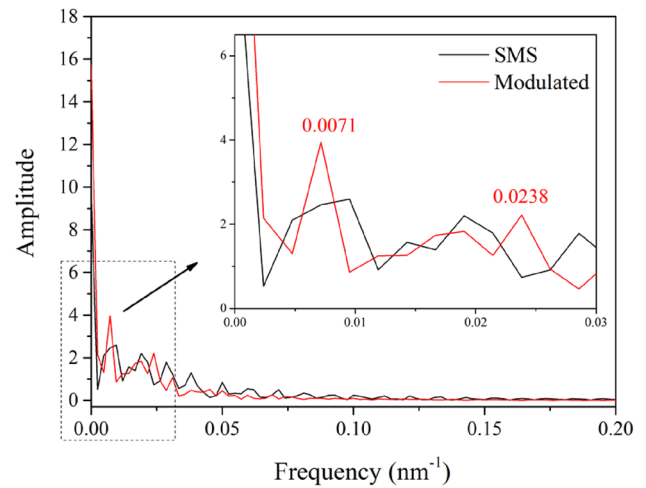

Fig. 4 Spatial frequency spectra on the SP-SMS and original SMS

which will induce a higher strain sensitivity. Additionally, when axial strain is applied to the fiber, microbending will be generated in the MMF core due to the spiral asymmetric structure. Hence, the refractive index difference of the MMF will change, which will increase the strain responses of the proposed sensor.

To investigate the mode distribution of the proposed structure, fast Fourier transform (FFT) of the SP-SMS and original SMS is performed in the spectral range of 1280 nm–1700 nm, as presented in Fig. 4. For the FFT spectrum of the SP-SMS, the spatial frequency spectrum shows some distinct peaks, which implies that the interference pattern contains the interference between the core mode and more than one kind of cladding mode, inducing different responses of the interference peaks to ambient perturbations, for instance, temperature variation and strain change. As a consequence, the sensor can be applied to simultaneously measure strain and temperature.

3 Measurement

Figure 5 shows a schematic diagram of the experimental setup for strain and temperature measurement of the proposed sensor. The spiral-polished SMS structure is fixed in the middle of two fiber fixtures, and the applied axial strain on the optical fiber structure can be realized by stepping the mobile stage, which is controlled by a motion controller. The variation in the axial strain is calculated by the following relationship:

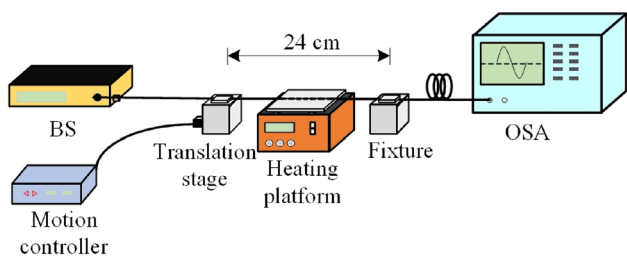$$\Delta\varepsilon = \frac{\Delta l}{l}, \tag{6}$$

Fig. 5 Experimental setup for measurement of the strain and temperature

where Δl is the step length of the two translation stages. l is the distance between the two fiber fixtures, which is 240 mm in this experiment.

In the strain measurement, the applied strain is set from 0 µε to 600 µε with a step of 50 µε. The wavelength evolution of the proposed structure under different axial strains is recorded by the OSA, as shown in Fig. 6a. Dip A and

Dip B exhibit blueshifts in the transmission spectrum from 1319.6 nm to 1309 nm and from 1359.8 nm to 1359.3 nm, respectively. Figure 6b shows the linear relation between the wavelengths of the two dips and the applied strain. The sensitivity of the proposed structure is calculated to be −17 pm/µε for Dip A and −1 pm/µε for Dip B.

In addition, to verify that the spiral-polished modulation has the ability to enhance the strain sensitivity of the sensor, strain characteristic measurement of the SMS structure with an MMF length of 2.5 cm is also performed, with the measurement method being consistent with the above method. Figure 7a shows the wavelength shift of the selected dip (near 1310 nm) in the transmission spectrum with increasing strain. The linear relation between the measured points and applied strain on the structure is shown in Fig. 7b. The strain sensitivities of the SMS are relatively low, i.e., −1.9 pm/µε and −1.5 pm/µε at 1311 nm and 1364 nm, respectively. It can be deduced that the design of the spiral structure effectively improves the strain response of the sensor.
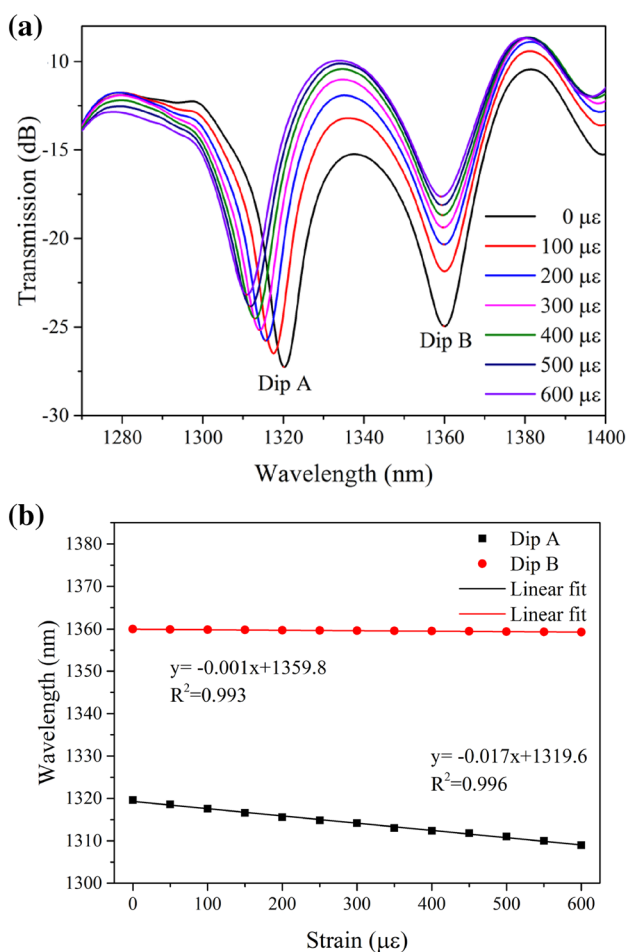

Fig. 6 Strain measurement of the sensor. **a** Dip A and Dip B exhibit blueshifts in the transmission spectrum with increasing axial strain. **b** Fitted curve of the relation between the wavelength and strain
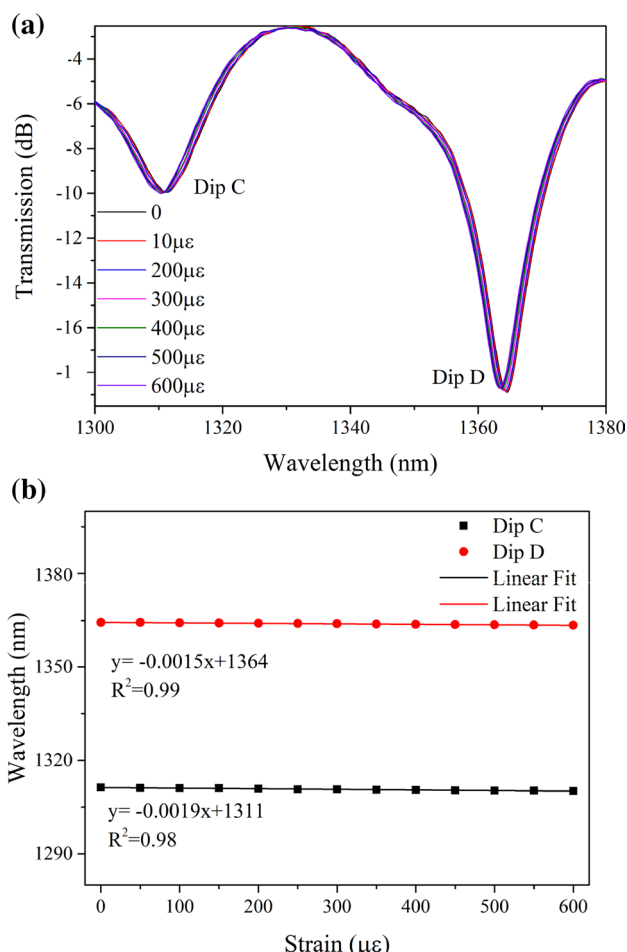

Fig. 7 Strain measurement of the original SMS structure. **a** Wavelength evolution of the structure with increasing strain. **b** Fitted curve of the relation between the wavelength and strain
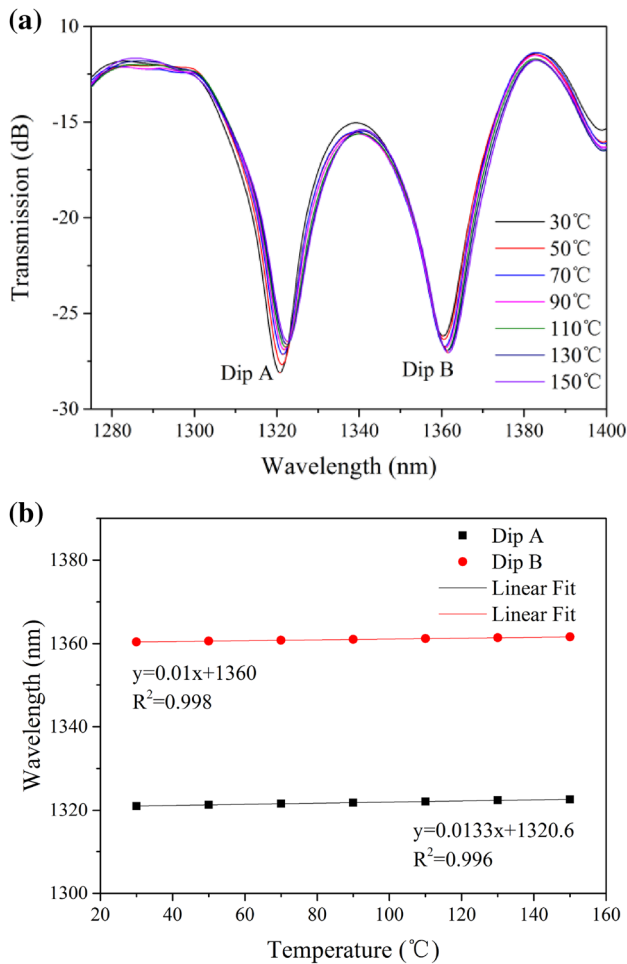
(a)

(b)

Fig. 8 Temperature characteristics of the sensor. **a** Dip A and Dip B exhibit a redshift in the transmission spectrum with increasing temperature. **b** Fitted curve of the relation between the wavelength and temperature

To investigate the effect of temperature variation on the strain measurement, a temperature measurement of the proposed sensor is performed. The external temperature of the fiber structure is changed by a constant temperature heating device. Figure 8a shows the temperature response of the sensor from 20 ℃ to 150 ℃ with a step of ~20 ℃. Dip A and Dip B exhibit redshifts from 1320.8 nm to 1322.6 nm and from 1360.2 nm to 1361.6 nm, respectively. The linear relation between the temperature and wavelength shift of the sensor is presented in Fig. 8b. The temperature sensitivities of the sensor are 10 pm/℃ and 13.3 pm/℃ for Dip A and Dip B, respectively.

On the basis of the experimental results mentioned above, simultaneous measurement of the strain and temperature can be realized by the sensor based on the fiber SP-SMS structure. When the external temperature and strain change simultaneously, the equation for simultaneous measurement of the sensor is expressed as:

$$
\begin{bmatrix} \Delta T \\ \Delta \varepsilon \end{bmatrix} = \frac{1}{D} \begin{bmatrix} S_{\varepsilon B} & -S_{\varepsilon A} \\ -S_{TB} & S_{TA} \end{bmatrix} \begin{bmatrix} \Delta \lambda_A \\ \Delta \lambda_B \end{bmatrix},
\tag{7}
$$

where $D = S_{\varepsilon B} S_{TA} - S_{\varepsilon A} S_{TB}$ and ΔT and $\Delta \varepsilon$ are the variations in the temperature and strain, respectively. S_ε is the strain sensitivity of Dip A ($S_{\varepsilon A}$) and Dip B ($S_{\varepsilon B}$), and S_T is the temperature sensitivity of Dip A (S_{TA}) and Dip B (S_{TB}). $\Delta \lambda_A$ and $\Delta \lambda_B$ are the wavelength shifts of Dip A and Dip B, respectively.

Under the current conditions, the strain and temperature resolutions of the sensor are calculated by:

$$
\begin{bmatrix} \Delta T \\ \Delta \varepsilon \end{bmatrix} = \frac{1}{2.16 \times 10^{-4}} \begin{bmatrix} -0.001 & 0.017 \\ -0.013 & 0.010 \end{bmatrix} \begin{bmatrix} \Delta \lambda_A \\ \Delta \lambda_B \end{bmatrix}.
\tag{8}
$$

From Eq. (6), the variation in the temperature and strain of the structure can be calculated. The resolutions of the spiral-polished fiber sensor are evaluated as ± 1.48 ℃ and ± 0.27 µε, respectively.

4 Conclusions

In summary, a novel fiber sensor for the simultaneous measurement of strain and temperature based on a spiral-polished SMS structure is developed. The geometrical shape of the spiral effectively enhances the strain sensitivity. Two noted dips (Dip A: 1319.6 nm; Dip B: 1359.8 nm) of the SP-SMS exhibit different strain sensing characteristics due to the different interference cladding modes. In the strain measurement experiment, the sensitivities of the two dips are −17 pm/µε and −1 pm/µε, respectively. In addition, the proposed fiber sensor has the ability to distinguish the temperature and strain simultaneously, with resolutions of ± 1.48 ℃ and ± 0.27 µε, respectively. Moreover, this sensor is low cost, is easy to fabricate and has a simple structure. Therefore, we believe that the spiral-polished SMS structure has potential in many sensing applications and offers a new way to realize the simultaneous measurement of strain and temperature.

Reference

1. J.M. Lopez-Higuera, L.R. Cobo et al., Fiber Optic Sensors in Structural Health Monitoring. J Lightw Technol **29**, 587–608 (2011)
2. B. Lee, Review of the present status of optical fiber sensors. Opt Fiber Technol **9**, 57–79 (2003)
3. J.Y. Lou, Y.P. Wang, L.M. Tong, Microfiber optical sensors: a review. Sensors **14**, 5823–5844 (2014)
4. Y. Zhao, R.J. Tong et al., Relative humidity sensor based on Vernier effect with GQDs-PVA un-fully filled in hollow core fiber Sens. Actuators A Phys **285**, 329–337 (2019)
5. X.Y. Zhong, Y.P. Wang, High-sensitivity strain sensor based on inflated long period fiber grating. Opt Lett **39**, 5463–5466 (2014)
6. R.J. Wu, B.L. Zheng et al., Study on strain transfer of embedded fiber Bragg grating sensors. Opt Eng. **53**, 8 (2014)
7. H.P. Gong et al., Strain sensor realized by using low-birefringence photonic-crystal-fiber-based sagnac loop. IEEE Photon Technol Lett **22**, 1238–1240 (2011)
8. Y.J. Rao et al., Novel fiber-optic sensors based on long-period fiber gratings written by high-frequency CO_2 laser pulses. J Lightw Technol **21**, 1320–1327 (2003)
9. Y. Sun et al., High sensitivity optical fiber strain sensor using twisted multimode fiber based on SMS structure. Opt Commun **405**, 416–420 (2017)
10. T. Saurabh, K. Arun et al., Strain and temperature sensing characteristics of single-mode-multimode-single-mode structures. J Lightw Technol **27**, 2348–2356 (2009)
11. X. Rui, C.B. Dong, Simultaneous strain and temperature sensor based on polarization maintaining fiber and multimode fiber. Opt Laser Technol **102**, 17–21 (2018)
12. Q. Wang, Investigation on single-mode–multimode–single-mode fiber structure. J Lightw Technol **26**, 512–519 (2008)
13. Y. Sun et al., Dual-parameters optical fiber sensor with enhanced resolution using twisted mmf based on SMS structure. IEEE Sens J **17**, 3045–3051 (2017)
14. R.N. Wang et al., Investigation on the polarization dependence of an angled polished multimode fibre structure. J Lightwave Technol **38**, 4520–4525 (2020)
15. Y.W. Ma et al., Torsion and temperature sensor based on polished MSM structure, IEEE photon. Technol Lett **32**, 1117–1120 (2020)
16. R. Yang et al., Single S-tapered fiber Mach-Zehnder interferometers. Opt Lett **39**, 4482–4484 (2011)